A single-cell atlas of alternative wing development in two hemipteran species

Yi Wan[1], Hui-Jie Wu, Heng-Guang Huang, Zhuo-Qi Liu, Zhao-Xiang Sun, Zhang-Nv Yang, Hai-Jun Xu

This Supplementary information includes:

Supplementary Figs. 1-13

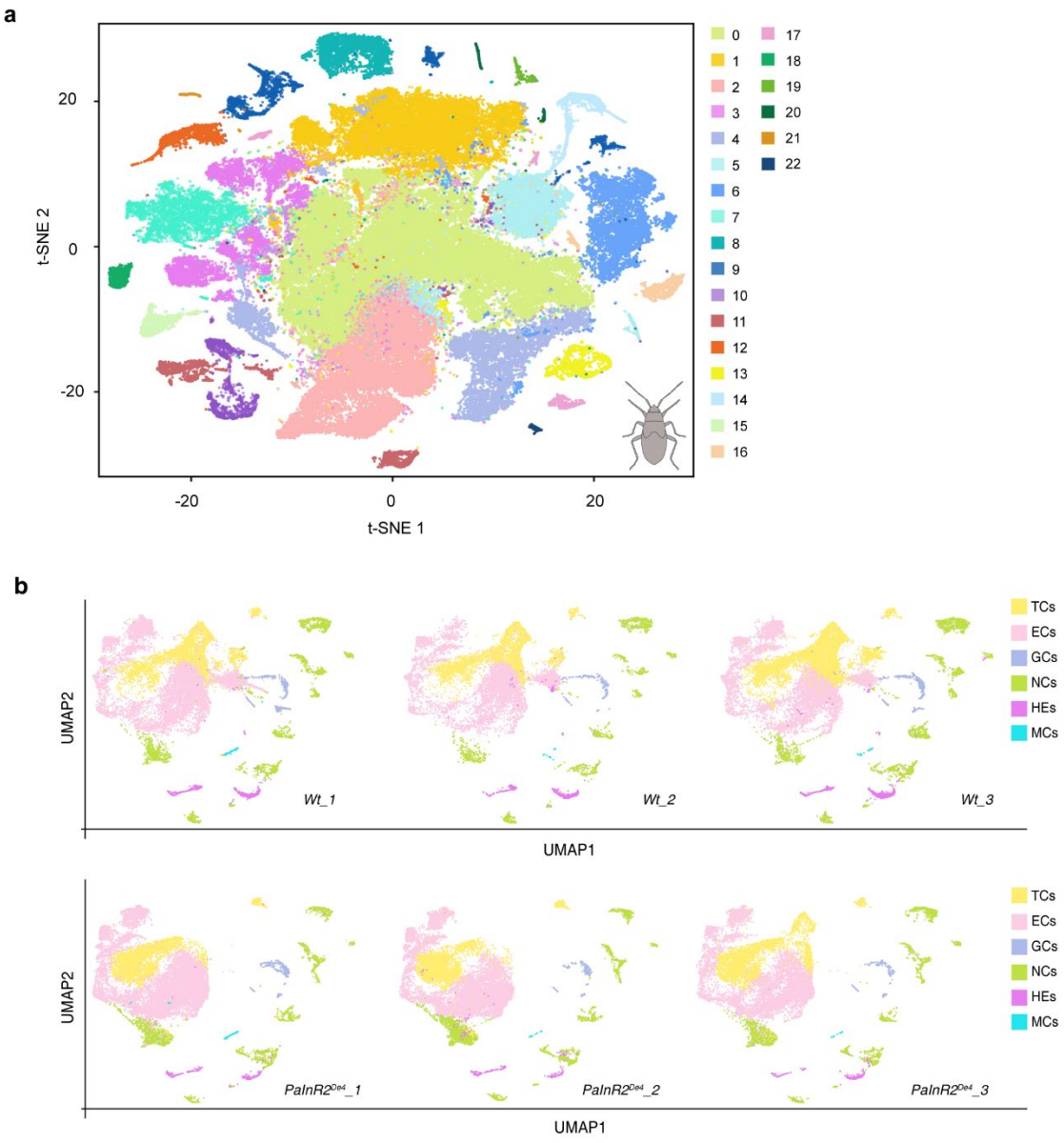

Supplementary Fig. 1. *Wt* and *PaInR2^{De4}* wing buds have an identical cell-type landscape. **a** t-SNE visualization of 23 cell clusters obtained from *Wt* and *PalInR2^{De4}* wing buds (resolution=0.2). Each dot represents one cell. **b** UMAP plots visualization of six major cell types in the wing buds across three independent biological replicates for both *Wt* and *PalInR2^{De4}* nymphs.

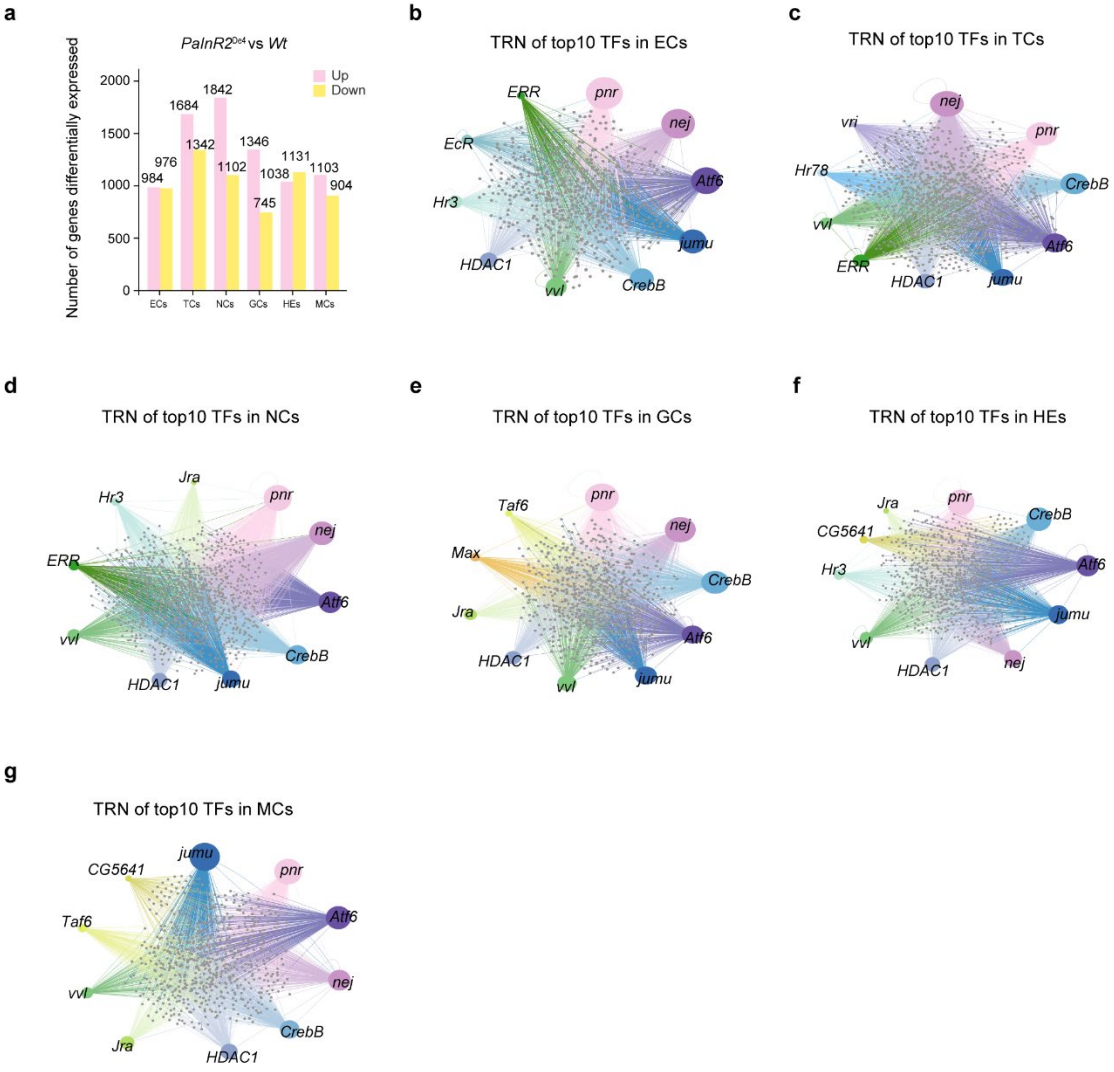

Supplementary Fig. 2. Subtle changes in transcriptional regulation among cell types in *PalInR2^{De4}* and *Wt* wing buds. a Bar plot showing the number of significantly up-regulated (pink) and down-regulated (yellow) differentially expressed genes (DEGs) across six major cell types of *PalInR2^{De4}* wing buds relative to *Wt*. **b-g** Visualization of transcriptional regulatory network (TRN) analyses for the top 10 candidate transcription factors (TFs) in ECs (**b**), TCs (**c**), NCs (**d**), GCs (**e**), HEs (**f**), and MCs (**g**). Within each network, peripheral nodes (colored) represent TFs, while central grey dots represent their respective DEG targets. The size of each TF node

scales with its regulatory degree, representing the number of DEGs it governs within the specific cell type. Source data are provided as a Source Data file.

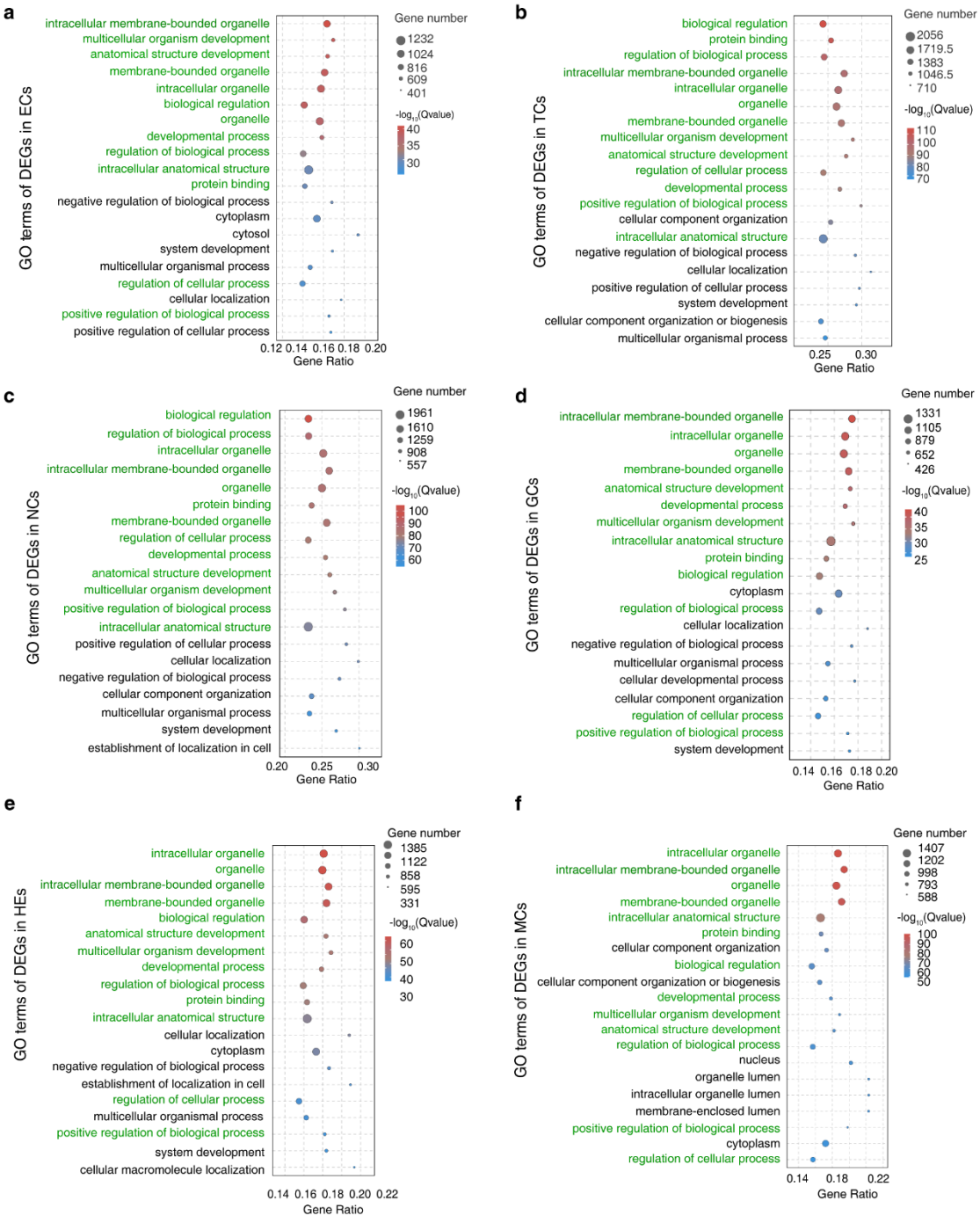

Supplementary Fig. 3. Six cell types have common Gene Ontology (GO) terms. **a-f** Dot plots of the top 20 functional categories enriched among differentially expressed genes (DEGs) that were identified in *PalInR2*^{De4} relative to *Wt* wing buds across six major cell types: EC (**a**), TC (**b**), NC (**c**), GC (**d**), HEs (**e**) and MC (**f**). The x-axis represents the Gene Ratio the proportion of DEGs within a given GO term, and

the y-axis lists specific GO terms. The color gradient represents statistical significance (presented as $-\log_{10}$(Q-value)). The dot size corresponds to the number of DEGs assigned to each term. GO terms highlighted in green indicate conserved functional categories enriched across all six cell types.

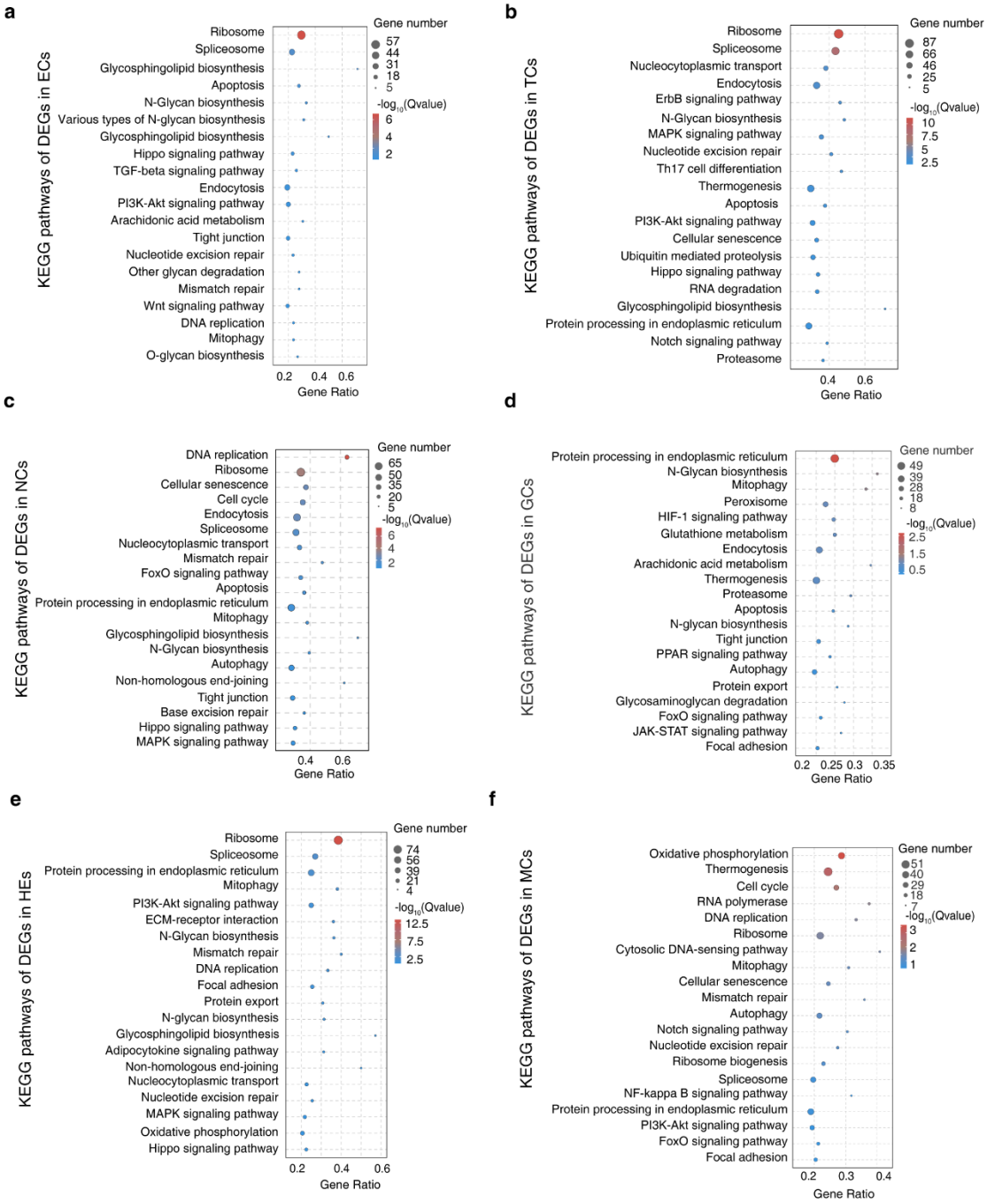

Supplementary Fig. 4. KEGG pathway enrichment analysis of cell-type-specific differentially expressed genes (DEGs) in wing buds. a – f Dot plots illustrating significantly enriched KEGG pathways for DEGs identified in *PalInR2*^{De4} relative to *Wt* wing buds within ECs (**a**), TCs (**b**), NCs (**c**), GCs (**d**), HEs (**e**), and MCs (**f**). The x-axis indicates the Gene Ratio. Dot size represents the number of DEGs associated

with each pathway, and the color gradient reflects statistical significance (presented as $-\log_{10}$(Q-value)).

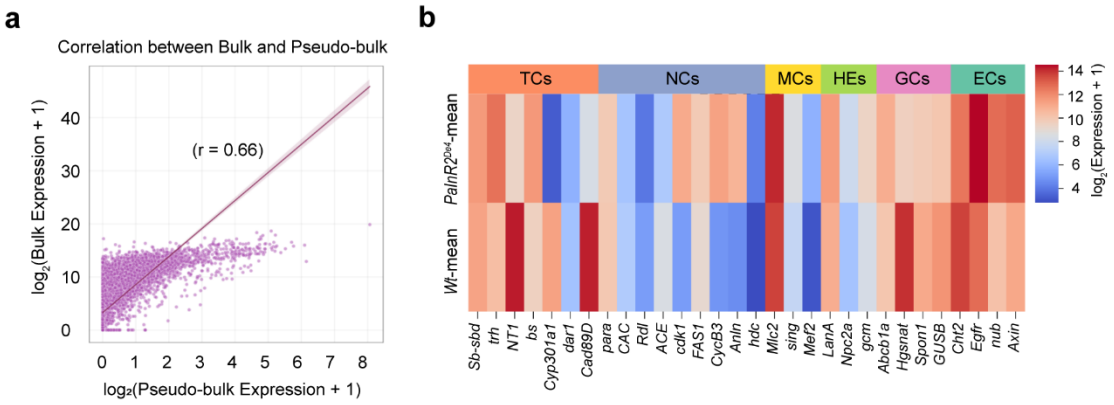

Supplementary Fig. 5. A high correlation between bulk-seq and scRNA-seq (pseudo-bulk) data in the firebug *P. apterus*. a A scatter plot of the comparison of log_2-transformed gene expression between scRNA-seq and bulk RNA-seq. Each dot represents the expression of one gene in pseudo-bulk profiles aggregated from scRNA-seq (x-axis) *vs* expression in bulk RNA-seq (y-axis). Pearson correlation, r = 0.66. **b** Heatmap of bulk RNA-seq expression for cell-type marker genes. Columns correspond to marker genes were grouped into six cell types (ECs, epithelial cells; TCs, tracheal cells; NCs, neuron cells; HEs, hemocytes; GCs, glial cell; MCs, muscle cells; top color bar), and rows show wing morph means from three independent biological replicates. Values, log_2(expression + 1).

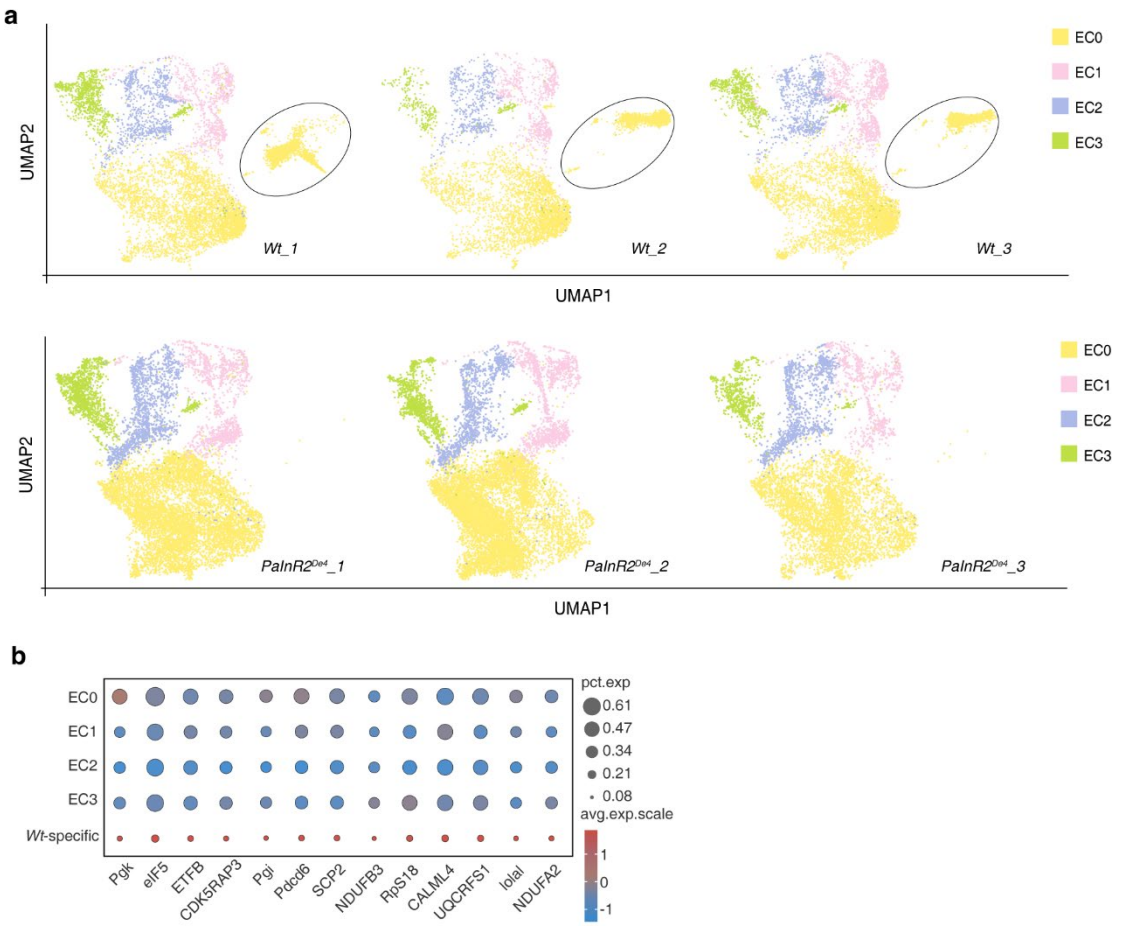

Supplementary Fig. 6. Characterization of a *Wt*-specific epithelial cell (EC) subcluster in wing buds. a UMAP visualizations of EC subclusters across three biological replicates of *Wt* and *PalInR2*^{De4} wing buds. A distinct cell population (circled) is present in three *Wt* replicates but absent in *PalInR2*^{De4}, designated as the *Wt*-specific cluster. EC0 – EC3 represent conserved epithelial subclusters identified in both genotypes. **b** Dot plot showing the expression profiles of representative marker genes for the *Wt*-specific cluster relative to EC0-EC3. The dot size represents the percentage of cells in the cluster expressing the gene (pct. exp.), and the color intensity demarks gene average expression level (avg. exp. scale).

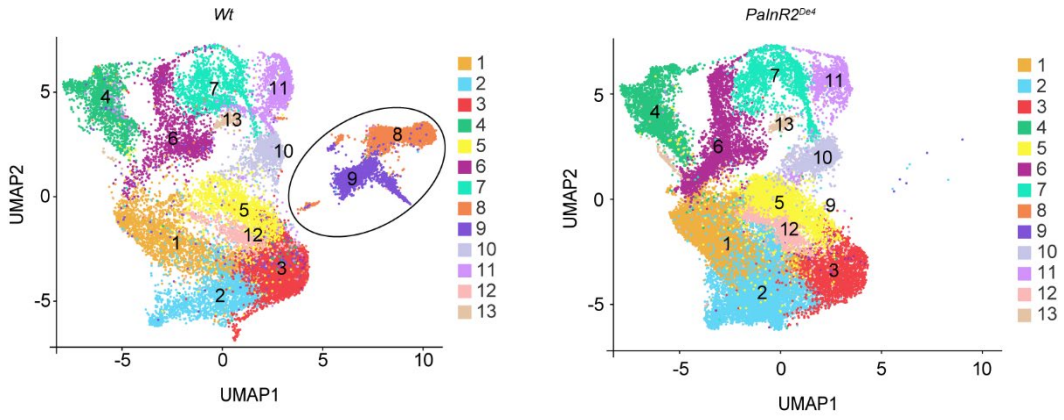

Supplementary Fig. 7. Analyses of *Wt*-specific epithelial cell (EC) subclusters under high resolution. UMAP visualizations of EC subclusters identified after integrating three biological replicates of *Wt* and *PalInR2*^{De4} wing buds, respectively (clustering resolution = 0.4). Cells are color-coded into 13 distinct subclusters (1 – 13). Subclusters 8 and 9 (circled) are prominently present in the *Wt* wing buds.

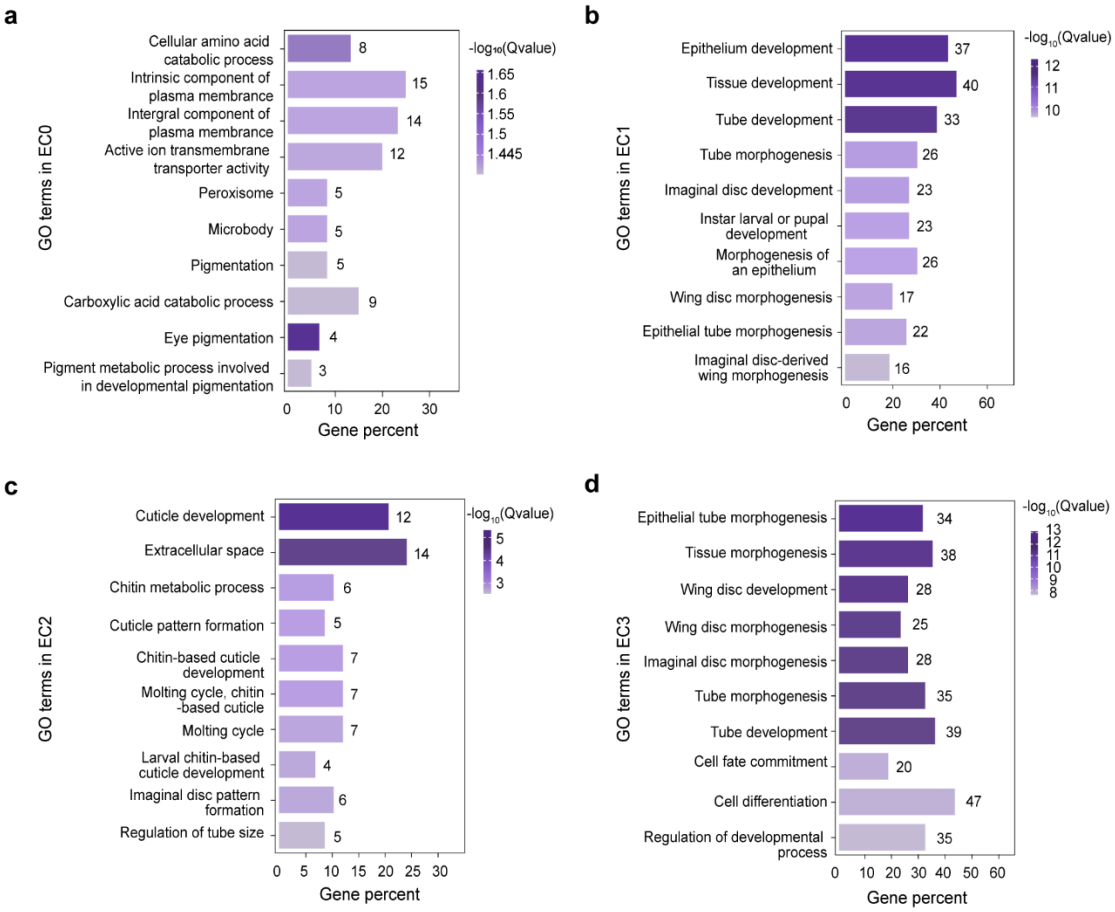

Supplementary Fig. 8. Gene Ontology (GO) enrichment analysis of epithelial cell (EC) subsets in wing buds of the firebug. Bar plots summarizing the functional categories enriched among up-regulated genes in EC0 (**a**), EC1 (**b**), EC2 (**c**), and EC3 (**d**) subclusters. The x-axis shows the proportion of up-regulated genes associated with each GO term, and the color gradient represents statistical significance (presented as $-\log_{10}$(Q-value)).

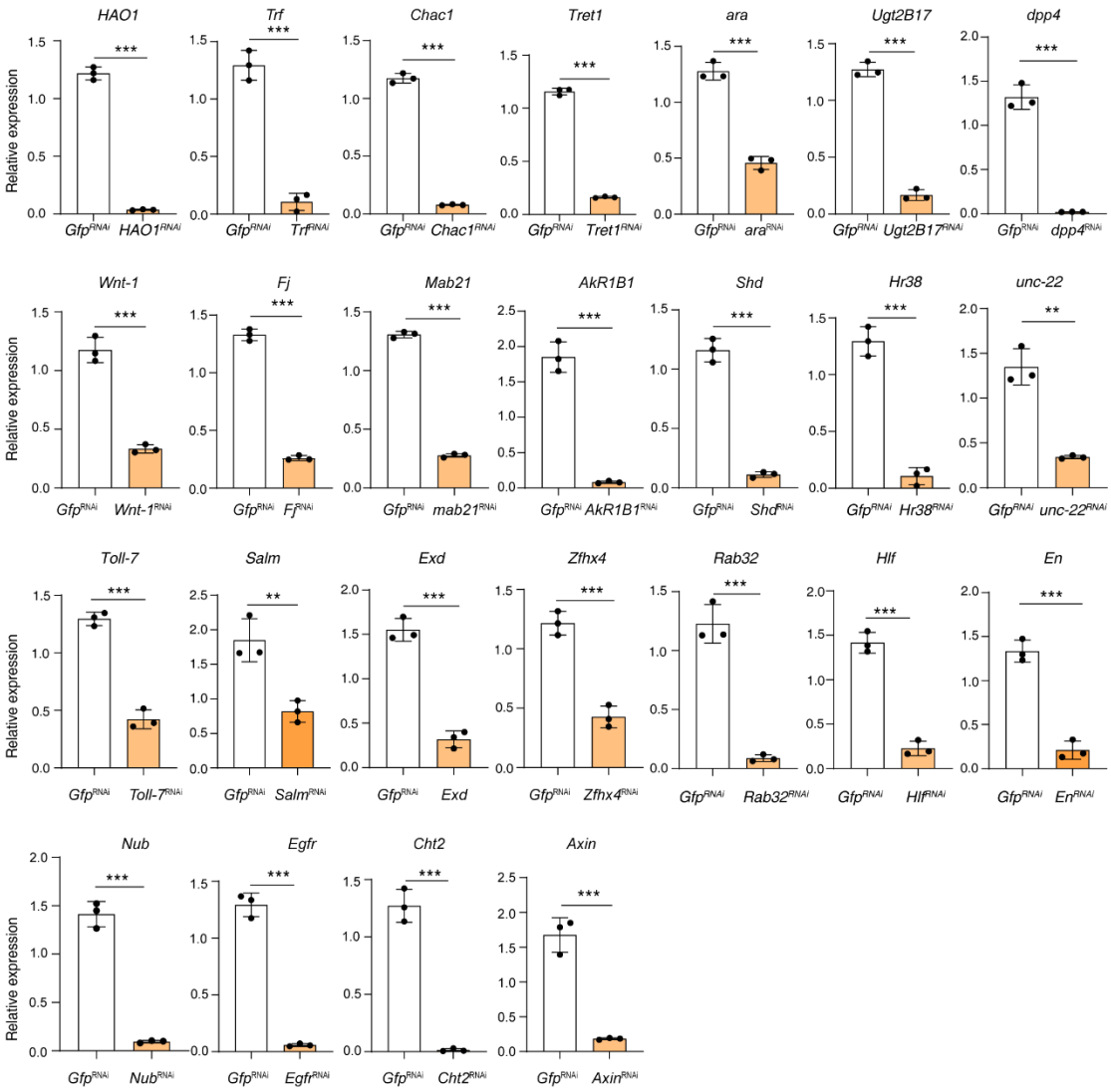

Supplementary Fig. 9. RNAi efficiency for EC marker genes. Total RNA was extracted from *Wt* nymphs injected with dsRNA targeting corresponding marker genes (orange bars) or *Gfp* as a control group (white bars), and then used for quantitative RT-PCR (qRT-PCR) analyses. Data represent the mean ± SD of three independent biological replicates (dots). Statistical significance was calculated by two-tailed Student's *t*-test (**$p < 0.01$; ***$p < 0.001$). Source data and exact *p* values are provided as a Source Data file.

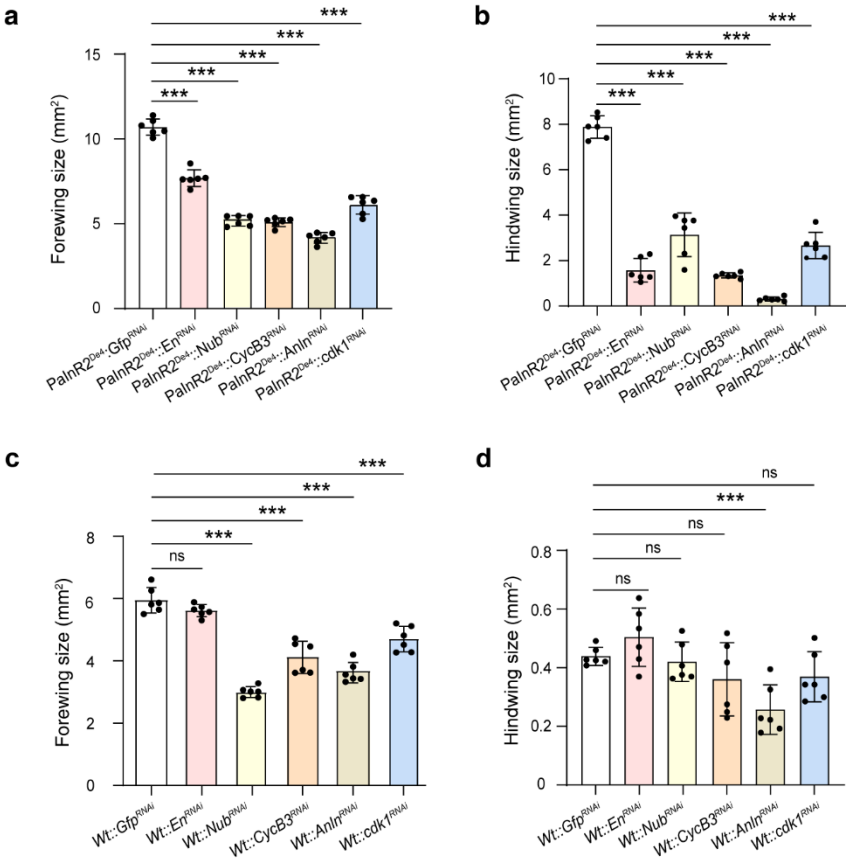

Supplementary Fig. 10. Quantification of wing size in *PaInR2^{De4}* and *Wt* after RNAi treatments. a Forewing size of *PaInR2^{De4}* adults after RNAi treatments. **b** Hindwing size of *PaInR2^{De4}* adults after RNAi treatments. **c** Forewing size of *Wt* adults after RNAi treatments. **d** Hindwing size of *Wt* adults after RNAi treatments. Knockdown of candidate genes (*En*, *Nub*, *CycB3*, *Anln*, and *cdk1*) was compared against control groups injected with *Gfp*-RNAi. Each dot represents an individual wing sample (n = 6 biological replicates). Bars represent mean ± SD. Statistical significance was determined using two-tailed Student's *t*-test comparing each treatment group to the respective *Gfp*-RNAi control (***$p < 0.001$; ns, not significant). Source data and exact *p* values are provided as a Source Data file.

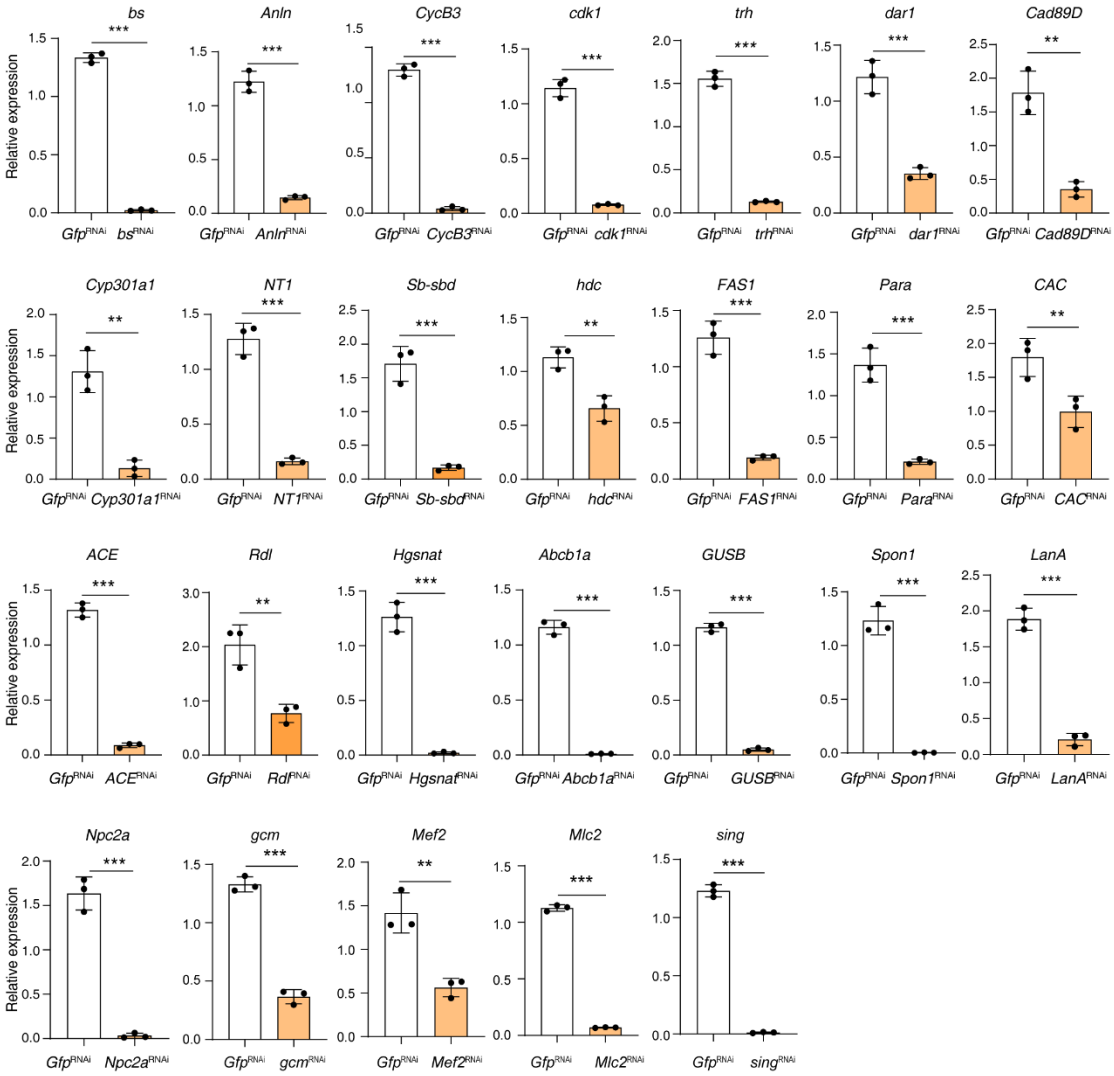

Supplementary Fig. 11. RNAi efficiency for TCs, NCs, GCs, HEs, and MCs marker genes. Total RNA was extracted from *Wt* nymphs injected with dsRNA targeting corresponding marker genes (orange bars) or *Gfp* as a control group (white bars), and then used for quantitative RT-PCR (qRT-PCR) analyses. Data represent the mean ± SD of three independent biological replicates (dots). Statistical significance was calculated by two-tailed Student's *t*-test (*$p < 0.05$; **$p < 0.01$; ***$p < 0.001$). Source data and exact *p* values are provided as a Source Data file.

Supplementary Fig. 12. Structural defects and blistering on the pronotum and scutellum following *bs* knockdown. Fifth-instar *Wt P. apterus* nymphs were collected for microinjection with dsRNA targeting *bs* gene. The RNAi treatment resulted in severe structural abnormalities and blistering on the pronotum (Pn) and scutellum (SI). Source data are provided as a Source Data file.

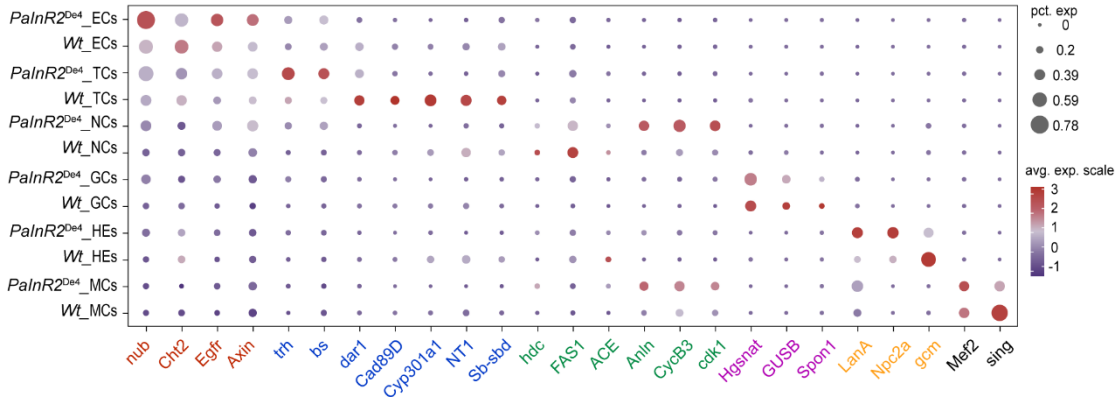

Supplementary Fig. 13. Differential expression of marker gene in each cell type of *Wt* and *PaInR2^{De4}*. The dot size represents the percentage of cells in the cluster expressing the gene (pct. exp.), and the color intensity demarks gene average expression level (avg. exp. scale).